Frontiers in Bioscience Landmark

Front. Biosci. (Landmark Ed) **2026**; 31(8): 54095
https://doi.org/10.31083/FBL54095

Original Research

Tazarotene-Induced Gene 2 Promotes Melanoma Cell Death via the Activation of Endoplasmic Reticulum Stress

Chun-Hua Wang[1,2], Lu-Kai Wang[3], Fu-Ming Tsai[4,*]

[1]Department of Dermatology, Taipei Tzu Chi Hospital, Buddhist Tzu Chi Medical Foundation, 231 New Taipei City, Taiwan
[2]School of Medicine, Tzu Chi University, 970 Hualien, Taiwan
[3]National Center for Biomodels, National Institutes of Applied Research, 115 Taipei, Taiwan
[4]Department of Research, Taipei Tzu Chi Hospital, Buddhist Tzu Chi Medical Foundation, 231 New Taipei City, Taiwan
*Correspondence: xd109061@tzuchi.com.tw; afu2215@gmail.com (Fu-Ming Tsai)
Academic Editor: Amancio Carnero Moya
Submitted: 21 May 2026 Revised: 7 July 2026 Accepted: 16 July 2026 Published: 21 August 2026

Abstract

Background: Tazarotene-induced gene 2 (*TIG2*), also known as retinoic acid receptor responder 2 (*RARRES2*), encodes the secreted protein TIG2, also known as chemerin, which is involved in immune regulation and metabolism. However, its role in melanoma remains unclear. **Methods:** *TIG2* expression was analyzed using The Cancer Genome Atlas, Genotype-Tissue Expression, OncoDB, and melanoma tissue cDNA arrays. To evaluate its effects on cell viability and death, TIG2 was overexpressed in A2058 and A375 melanoma cells. RNA sequencing (RNA-seq), qPCR, and Western blotting were performed to identify TIG2-regulated genes and signaling pathways. The involvement of chemokines and endoplasmic reticulum (ER) stress was further examined using the C-X-C motif chemokine ligand 10 (CXCL 10)/CXCL11 and the ER stress inhibitor tauroursodeoxycholic acid (TUDCA). **Results:** *TIG2* expression was reduced in melanoma and other skin cancers. TIG2 overexpression significantly reduced cell viability and induced cell death. RNA-seq analysis showed that TIG2 downregulated *CXCL10*, *CXCL11*, and *CCL2* while upregulating ER stress-related genes such as *HERPUD1* and *DDIT3*. Exogenous CXCL10 or CXCL11 did not reverse TIG2-mediated effects, whereas TUDCA partially restored cell viability and reduced cell death. **Conclusions:** These findings suggest that TIG2 suppresses melanoma cell growth by activating ER stress and modulating immune-related chemokines, highlighting its potential therapeutic relevance.

Keywords: TIG2; chemerin; CXCL10; CXCL11; ER stress; melanoma

1. Introduction

Tazarotene-induced gene 2 (*TIG2*), also known as retinoic acid receptor responder 2 (*RARRES2*), encodes the secreted protein TIG2 (chemerin) and was originally identified as a retinoic acid–inducible gene. The human *RARRES2* gene is located on chromosome 7q36.1, spans approximately 18 kb of genomic DNA, and encodes an ~0.8 kb mRNA transcript that translates into a 163-amino-acid secreted protein precursor [1,2]. The chemerin precursor requires C-terminal proteolytic processing to generate its biologically active form, which exerts its physiological functions by binding to chemokine-like receptor 1 (CMKLR1), G protein-coupled receptor 1, and the atypical chemokine receptor C-C motif chemokine receptor-like 2 [3]. Previous studies have demonstrated that TIG2/chemerin is widely expressed in adipose, liver, lung, and skin tissues, where it participates in adipogenesis, glucose metabolism, inflammatory responses, and immune cell chemotaxis [4,5].

Recent studies have further revealed that TIG2/chemerin is not only involved in metabolic regulation but is also closely associated with tumor progression and modulation of the immune microenvironment. TIG2 functions within the immune system as a chemotactic factor that recruits CMKLR1-expressing dendritic cells, macrophages, and natural killer (NK) cells to sites of inflammation or tumor lesions [2,6]. TIG2 expression exhibits tissue-specific and context-dependent patterns during tumor progression in various cancer types. For instance, reduced TIG2 expression has been observed in hepatocellular carcinoma, breast cancer, and melanoma, where it is often considered to exert tumor-suppressive effects [7,8,9]. In contrast, TIG2 expression has been associated with tumor progression and inflammatory responses in certain malignancies such as gastric and lung cancer [10,11]. Moreover, Pachynski et al. [8] reported that TIG2 can suppress melanoma growth by promoting NK cell infiltration into the tumor microenvironment, highlighting its dual roles in immune regulation and antitumor activity. However, whether TIG2 directly regulates cancer cell survival, cellular stress responses, and cell death mechanisms remains unclear.

Melanoma is an aggressive type of skin cancer derived from melanocytes. Although the incidence of melanoma is lower than that of basal and squamous cell carcinomas, it is characterized by high metastatic potential and significant mortality [12,13,14]. Prolonged exposure to ultraviolet radiation is a major risk factor for the development of melanoma, because of its induction of DNA damage, ox-

Copyright: © 2026 The Author(s). Published by IMR Press.
This is an open access article under the CC BY 4.0 license.

Publisher's Note: IMR Press stays neutral with regard to jurisdictional claims in published maps and institutional affiliations.

idative stress, and oncogenic mutations [15]. Genetically, mutations in the B-Raf proto-oncogene, serine/threonine kinase (BRAF), NRAS proto-oncogene, GTPase, and KIT proto-oncogene receptor tyrosine kinase are closely associated with melanoma progression, with $BRAF^{V600E}$ being the most common driver mutation [16]. Although BRAF and immune checkpoint inhibitors have significantly improved the outcomes of patients with advanced melanoma, therapeutic resistance and tumor recurrence remain major clinical challenges [17,18,19,20]. Therefore, elucidating the molecular mechanisms underlying melanoma progression and identifying novel therapeutic targets are critical.

Retinoids are derivatives of vitamin A that regulate cell differentiation, proliferation, and apoptosis by activating retinoic acid receptors and retinoid X receptors. Consequently, they have been widely investigated for the treatment of dermatological diseases and cancer [21]. Tazarotene, a third-generation retinoid, has been shown to inhibit skin tumor formation and suppress melanoma cell growth [22,23]. Previous studies have demonstrated that tazarotene induces the expression of multiple tazarotene-induced genes (TIGs), including *TIG1*, *TIG2*, and *TIG3*, which are thought to contribute to retinoid-mediated tumor suppression [1,24]. Among these, TIG1 has been reported to inhibit melanoma cell growth by regulating the VAC14 component of the PIKFYVE complex/mammalian target of rapamycin pathway and inducing endoplasmic reticulum (ER) stress [25,26]. Moreover, TIG3 has been shown to induce apoptosis by downregulating inhibitors of apoptosis proteins and activating caspase-3 [27]. In contrast, although TIG2 has been implicated in immune regulation, its direct role in melanoma cell survival and the underlying molecular mechanisms remain largely unknown.

The aim of this study was therefore to investigate the biological function and molecular mechanisms of TIG2 in melanoma. First, we examined the expression of *TIG2* in skin cancer tissues and melanoma cell lines. We then evaluated the effect of TIG2 overexpression on cell viability and death. Furthermore, we performed RNA sequencing (RNA-seq) to identify the downstream genes and signaling pathways regulated by TIG2, followed by molecular validation to explore their association with chemokine regulation and ER stress. Our findings demonstrate that TIG2 not only contributes to ER stress responses in melanoma cells but may also modulate tumor-associated immune factors, thereby influencing melanoma progression. These results provide new insights into TIG2 as a potential therapeutic target in melanoma.

2. Materials and Methods

2.1 Gene Expression Analysis in Human Melanoma Tissues

The expression of *TIG2* (*RARRES2*) in human melanoma tissues was examined using a commercially available melanoma tissue cDNA array (MERT301; OriGene Technologies, Rockville, MD, USA). This array was comprised of cDNA prepared from three normal skin specimens and 43 malignant melanoma tissues.

Quantitative real-time PCR was performed using *TIG2*-specific primers (forward: 5′-GAGGGACTGGAAGAAACCCG-3′; reverse: 5′-CCTTGGAGAAGGCGAACTGT-3′). β-actin primers supplied with the array kit were used as the endogenous reference. PCR amplification and data analysis were carried out as previously reported [28], with relative TIG2 expression calculated after normalization to β-actin.

2.2 Cell Culture, Plasmid Transfection, and Cell Line Authentication

Human melanoma A2058 (BCRC No. 60240) and A375 (BCRC No. 60263) cells were obtained from the Bioresource Collection and Research Center (BCRC, Hsinchu, Taiwan) and cultured at 37 °C in a humidified atmosphere containing 5% CO_2 in Dulbecco's modified Eagle's medium (DMEM; 90%) supplemented with 4 mM L-glutamine, 1.5 g/L sodium bicarbonate, 4.5 g/L glucose, 1 mM sodium pyruvate, and 10% fetal bovine serum, as described previously [25]. The expression plasmids TIG2-C-Myc (HG10361-CM), C-X-C motif chemokine ligand (CXCL)10-N-Flag (HG10768-NF), and CXCL11-C-Flag (HG10876-CF) were purchased from Sino Biological (Beijing, China).

Transient gene overexpression was achieved using Lipofectamine RNAiMAX (Invitrogen, Carlsbad, CA, USA). Cells were seeded into either 6-cm culture dishes (1×10^6 cells/dish) or 6-well plates (1×10^5 cells/well) and allowed to attach overnight before transfection. Plasmid DNA (3 µg per 6-cm dish or 1 µg per well of a 6-well plate) was diluted in Opti-MEM and mixed with Lipofectamine RNAiMAX at a ratio of 4 µL reagent per 1 µg DNA. After incubation at room temperature for 15 min, the DNA-lipid complexes were applied directly to the cells for four hours. The transfection medium was then replaced with complete growth medium, and the cells were cultured for an additional 24–48 h before subsequent analyses.

To facilitate reproducibility, different culture formats were used according to the downstream application. Six-centimeter dishes were used for experiments requiring relatively large amounts of RNA or protein, including RNA sequencing, Western blotting, and caspase-3 activity assays, whereas 6-well plates were used for cell viability assays, cytotoxicity assays, and quantitative real-time PCR analyses.

Unless otherwise specified, molecular analyses were performed 24 h after transfection, whereas cell viability and cytotoxicity were assessed 24–48 h after transfection, as indicated in the corresponding figure legends.

Cell line authentication was performed by short tandem repeat (STR) profiling, and the resulting profiles were matched with the DSMZ reference database [26]. To en-

sure the quality of cell cultures, the cells were routinely examined for mycoplasma contamination using both DAPI fluorescence staining and a commercial PCR-based detection kit (Cat. No. G239, Applied Biological Materials Inc., Richmond, BC, Canada).

2.3 Assessment of Cell Viability and Cytotoxicity Assays

Cell viability and cytotoxicity were evaluated as previously reported [26], with minor modifications. Briefly, A2058 and A375 cells were seeded at 1×10^5 cells per well in 6-well plates containing Dulbecco's modified Eagle's medium supplemented with 10% fetal bovine serum (FBS) and cultured overnight. Under these conditions, cells reached approximately 50–60% confluence at the time of transfection.

To evaluate the biological effects of TIG2 alone, cells were transfected with either an empty vector or a TIG2-C-Myc plasmid (1 µg/well). For the rescue experiments involving CXCL10 or CXCL11, four experimental groups were established: (1) empty vector control, (2) TIG2-C-Myc alone, (3) TIG2-C-Myc plus CXCL10-N-Flag, and (4) TIG2-C-Myc plus CXCL11-C-Flag. The total amount of plasmid DNA was kept to 1 µg per well by supplementing with the corresponding empty vector when necessary. For experiments examining the contribution of ER stress, cells were transfected with either the empty vector or TIG2-C-Myc plasmid and subsequently treated with 500 µM tauroursodeoxycholic acid (TUDCA; Sigma-Aldrich, St. Louis, MO, USA; Cat. No. T0266). TUDCA stock solution was prepared in ethanol (EtOH), and the working concentration was made by adding 5 µL of stock solution per mL of culture medium. Vehicle-treated control cultures received an equal volume of EtOH (5 µL/mL).

Following transfection, the culture medium was replaced with fresh medium containing 1% FBS, with or without 500 µM TUDCA, and cells were incubated for an additional 24–48 h before analysis.

Cell viability was determined using the WST-1 assay (Roche Diagnostics, Mannheim, Germany; Cat. No. 11644807001). After incubation with WST-1 reagent for 4–6 h, absorbance was measured using an Enzyme Immunoassay (EIA) microplate reader (Infinite F200; Tecan, Männedorf, Switzerland), and mitochondrial metabolic activity was expressed relative to the control group. Cytotoxicity was evaluated by quantifying the release of lactate dehydrogenase (LDH) using a Cytotoxicity Detection Kit (Roche Diagnostics; Cat. No. 11644793001) according to the manufacturer's instructions.

2.4 RNA-seq and Bioinformatic Analysis

A2058 melanoma cells were transiently transfected with either the TIG2-C-Myc expression plasmid or the corresponding empty vector control. At 24 h after transfection, total RNA was isolated using TRIzol reagent (Invitrogen, Carlsbad, CA, USA; Cat. No. 15596026) following the manufacturer's instructions. RNA quality was verified prior to sequencing, and the samples were submitted to the Biotools Microbiome Research Center (Taipei, Taiwan) for library preparation, high-throughput RNA sequencing, and downstream bioinformatic analysis.

Raw sequencing reads underwent quality assessment and trimming using Trimmomatic to remove adaptor sequences and low-quality bases. The filtered reads were subsequently aligned to the human reference genome using HISAT2, and gene-level read counts were generated with featureCounts. Expression values were normalized using the Relative Log Expression (RLE), Trimmed Mean of M-values (TMM), and Fragments Per Kilobase of transcript per Million mapped reads (FPKM) methods. Differential expression analysis was performed with DESeq2 based on three independent biological replicates. Genes meeting the criteria of an absolute fold change >2 together with an adjusted p-value < 0.05 were considered to be significantly differentially expressed.

2.5 Quantitative Real-Time PCR

Gene expression changes identified by RNA-seq were further validated by quantitative real-time PCR (qRT-PCR). Unless otherwise specified in the Results section, A2058 and A375 melanoma cells were transfected with either the empty vector or the TIG2-C-Myc expression plasmid and harvested 24 h later.

Total RNA was extracted using TRIzol reagent (Invitrogen) and reverse-transcribed into complementary DNA using the GScript RTase Kit (GeneDireX, Taoyuan, Taiwan; Cat. No. MB303-0050) according to the manufacturer's protocol. Quantitative PCR amplification was performed as described previously [25].

Primer sequences used for PCR of homocysteine-inducible ER protein with ubiquitin-like domain 1 (*HERPUD1*), DNA damage-inducible transcript 3 (*DDIT3*), *HSPA5*, and *HSPA6* were the same as reported previously [26], whereas the primers designed for *CXCL10*, *CXCL11*, *CCL2*, *IFIT1*, *IFIT2*, *IFNB1*, and *RPLP0P2* are listed below:

CXCL10: Forward 5′-TGCTGCCTTATCTTTCTGACTC-3′; Reverse 5′-TGCATCGATTTTGCTCCCC-3′

CXCL11: Forward 5′-TTCCACTGCCCAAAGGAGTC-3′; Reverse 5′-TGTCTCCACCGTAACCACAG-3′

CCL2: Forward 5′-CTTCATTCCCCAAGGGCTCG-3′; Reverse 5′-GTCTTCGGAGTTTGGGTTTGC-3′

IFIT1: Forward 5′-GAGGAGCCTGGCTAAGCAAA-3′; Reverse 5′-GGCTTCCTCATTCTGGCCTT-3′

IFIT2: Forward 5′-CCTGCCGAACAGCTGAGAAT-3′; Reverse 5′-CTGCCTCGTTTTGCCCTTTG-3′

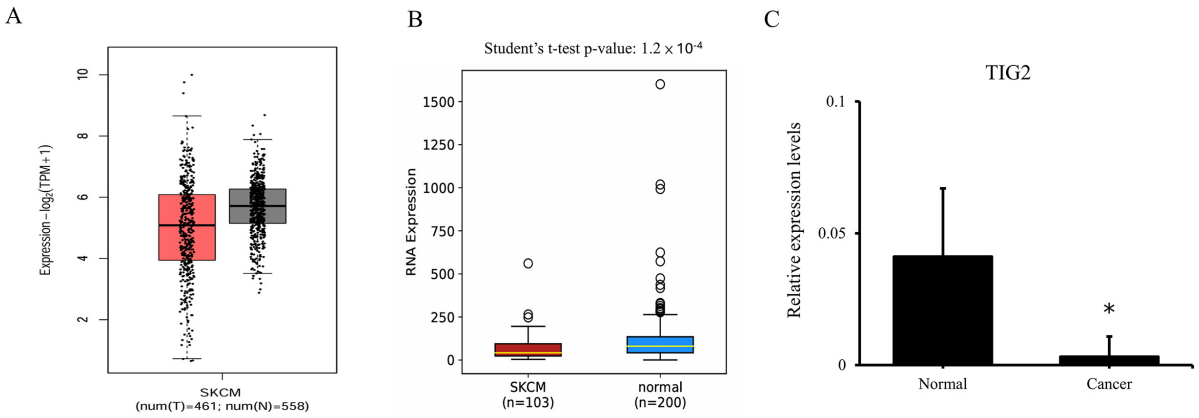


Fig. 1. Reduced tazarotene-induced gene 2 (*TIG2*) expression in melanoma tissues. *TIG2* transcript levels were compared between normal skin and melanoma tissues using the Cancer Genome Atlas (TCGA) (A) and OncoDB (B) databases. TIG2 mRNA expression was further validated by quantitative real-time PCR using a commercially available melanoma tissue cDNA array (MERT301) (C). Data are presented relative to normal skin tissues. *$p < 0.05$ versus normal skin.

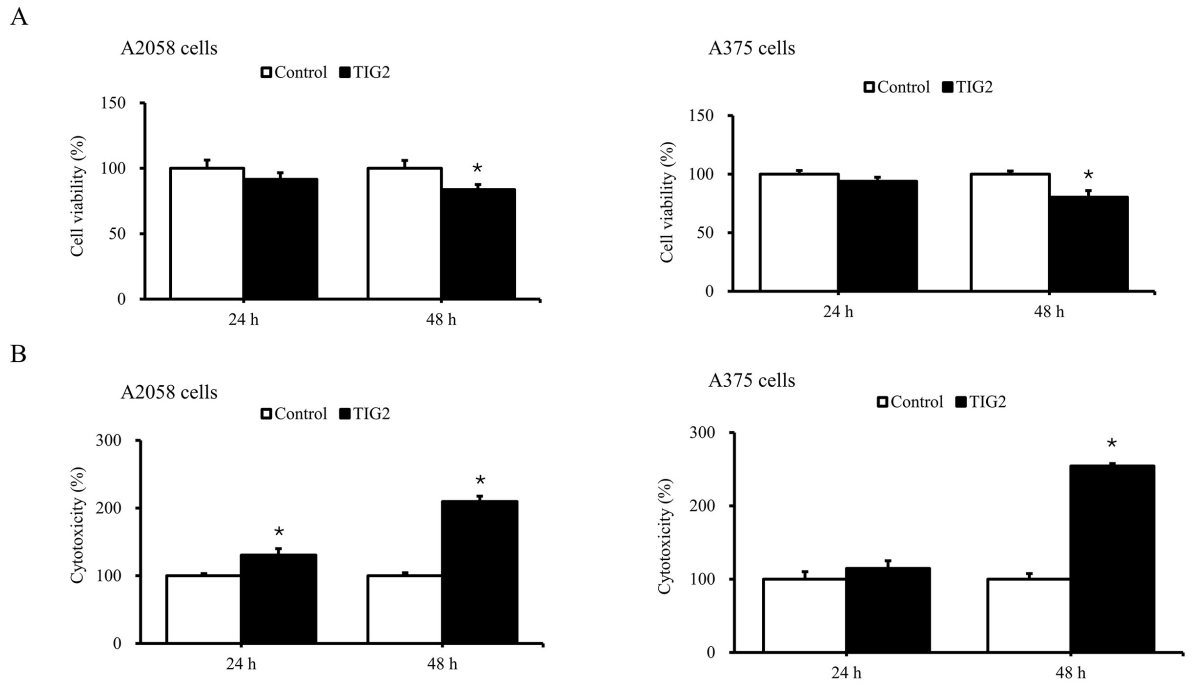


Fig. 2. TIG2 overexpression suppresses melanoma cell growth and promotes cell death. A2058 and A375 melanoma cells were transiently transfected with either an empty vector or the TIG2-C-Myc expression construct. Cell metabolic activity was determined using the WST-1 assay (A), and cytotoxicity was quantified by measuring lactate dehydrogenase (LDH) release (B) at the indicated time points. The data represent three independent experiments. *$p < 0.05$ versus control.

IFNB1: Forward 5′-GCGACACTGTTCGTGTTGTC-3′; Reverse 5′-GCGTCCTCCTTCTGGAACTG-3′

RPLP0P2: Forward 5′-GAAGCCAAGGAAGAGTCGGA-3’; Reverse 5′-GTCACAACCGTGGGAGCAAG-3′. Relative mRNA expression was calculated after normalization to β-actin, which served as the internal reference gene.

2.6 Immunoblot Analysis

Following the indicated treatments, cells were washed with cold phosphate-buffered saline and lysed in RIPA buffer supplemented with a protease inhibitor cocktail (Roche Diagnostics, Mannheim, Germany; Cat. No. 4693116001) and phosphatase inhibitor mixture. Total protein concentrations were determined using a bicinchoninic acid (BCA) protein assay kit (Thermo Fisher Scientific, Waltham, MA, USA; Cat. No. A55860).

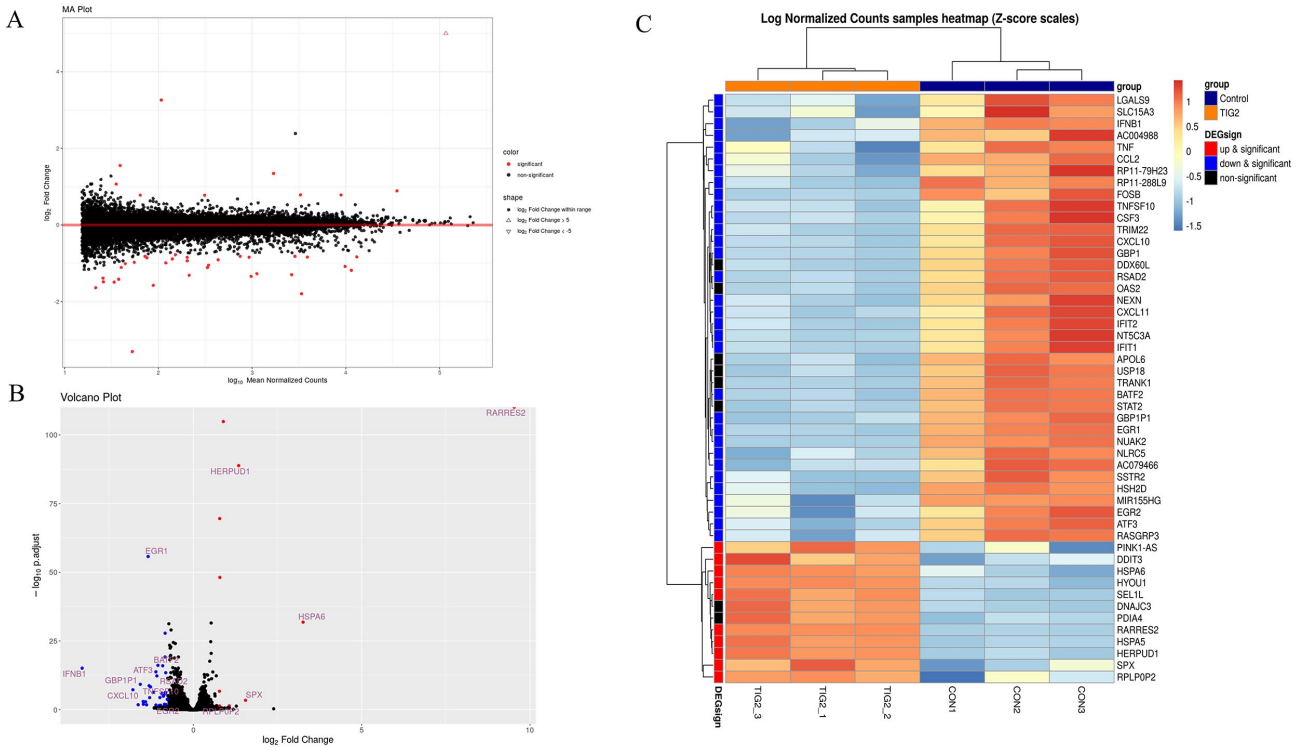


Fig. 3. Transcriptomic profiling of TIG2-overexpressing melanoma cells. RNA sequencing was performed on A2058 cells expressing either the empty vector or TIG2-C-Myc for 24 h. Differential gene expression is illustrated by an MA plot (A), and a volcano plot that highlights upregulated (red) and downregulated (blue) transcripts (B). Genes exhibiting greater than two-fold expression changes are summarized in the heatmap (C).

Equivalent amounts of protein were separated by sodium dodecyl sulfate-polyacrylamide gel electrophoresis and transferred onto polyvinylidene difluoride membranes. After blocking with non-fat milk, membranes were incubated overnight at 4 °C with the appropriate primary antibodies, followed by incubation with horseradish peroxidase-conjugated secondary antibodies. Immunoreactive bands were visualized using an enhanced chemiluminescence detection system according to the manufacturer's recommendations.

Primary antibodies against β-actin, MYC, and FLAG were as reported previously [28]. Antibodies against CXCL10 (10H11L3) and CXCL11 (PA5-104147) were purchased from Invitrogen (Carlsbad, CA, USA), antibodies against HERPUD1 (CST#26730) and CCL2 (CST#23236) from Cell Signaling Technology (Danvers, MA, USA), and the antibody against DDIT3 (CHOP) from Abclonal (Woburn, MA, USA; Cat. No. A20987). Horseradish peroxidase-conjugated secondary antibodies were obtained from Sigma-Aldrich (St. Louis, MO, USA). Protein expression levels were quantified by densitometric analysis and normalized to β-actin.

2.7 Caspase-3 Activity Assay

To determine whether TIG2-induced cell death was associated with activation of the apoptotic pathway, caspase-3 enzymatic activity in A2058 and A375 melanoma cells was measured following plasmid transfection. Briefly, cells were transfected with either the empty vector or the TIG2-C-Myc expression plasmid and cultured for the indicated time periods. After treatment, the cells were harvested and lysed in RIPA buffer. Equal amounts of total cellular protein were incubated in a reaction buffer containing 25 mM HEPES (pH 7.5), 0.1% CHAPS, 5% sucrose, 5 mM dithiothreitol (DTT), 2 mM EDTA, and 2 mM of the colorimetric caspase-3 substrate Ac-DEVD-p-nitroanilide (Ac-DEVD-pNA; Sigma-Aldrich; Cat. No. A2559). The reaction mixtures were incubated at 37 °C until color development was sufficient for detection.

Cleavage of Ac-DEVD-pNA was quantified by measuring absorbance at 405 nm using a microplate reader (Infinite F200). Caspase-3 activity was expressed as the relative absorbance normalized to the corresponding control group.

2.8 Statistical Analysis

All experiments were independently repeated at least three times to ensure reproducibility. Quantitative data are presented as the mean ± standard deviation (SD). Statistical analyses were carried out using GraphPad Prism software (version 11; GraphPad Software, San Diego, CA, USA).

Comparisons among multiple experimental groups were performed using one-way analysis of variance

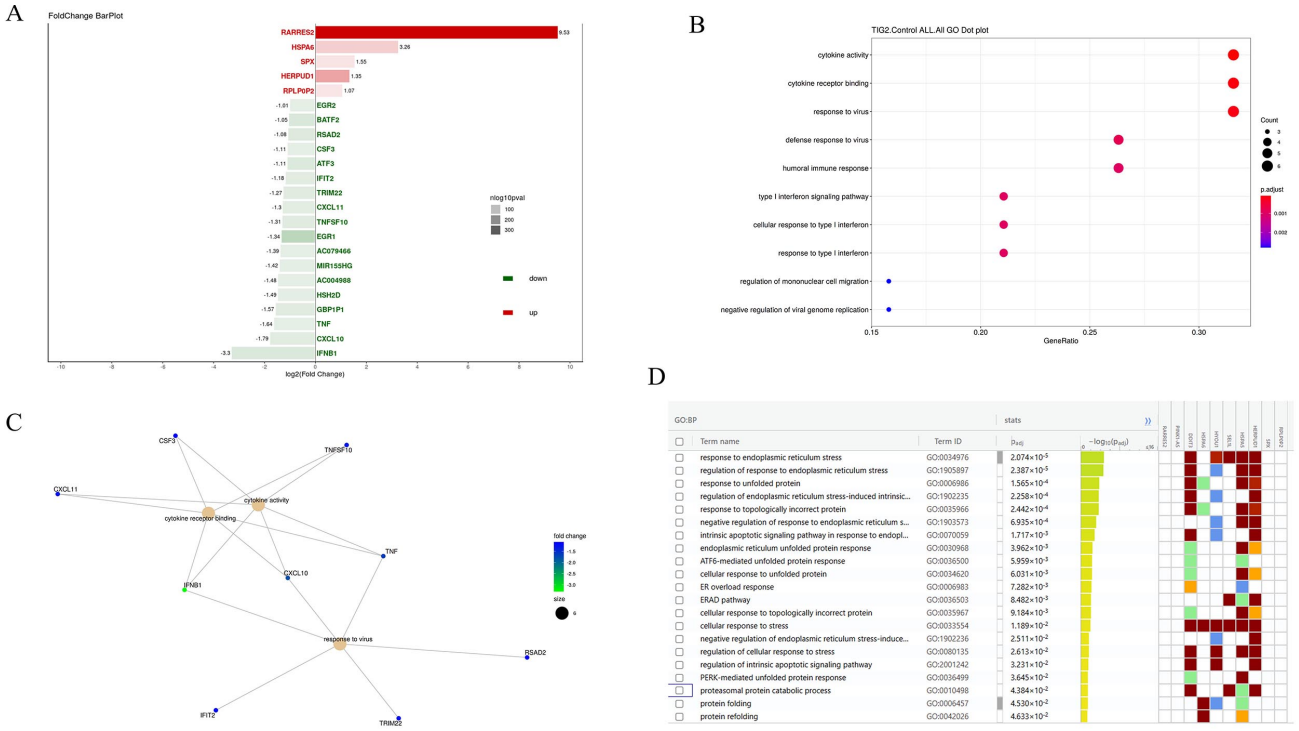


Fig. 4. Functional enrichment analysis of genes regulated by TIG2. Differentially expressed genes identified by RNA-seq were subjected to functional enrichment analyses. The distribution of significantly altered genes is shown as a bar plot (A). Gene Ontology (GO) enrichment analysis identified several biological processes associated with TIG2-regulated genes (B), including cytokine activity, receptor binding, and antiviral responses (C). The enriched GO biological processes among TIG2-upregulated genes were further analyzed using g:Profiler (D).

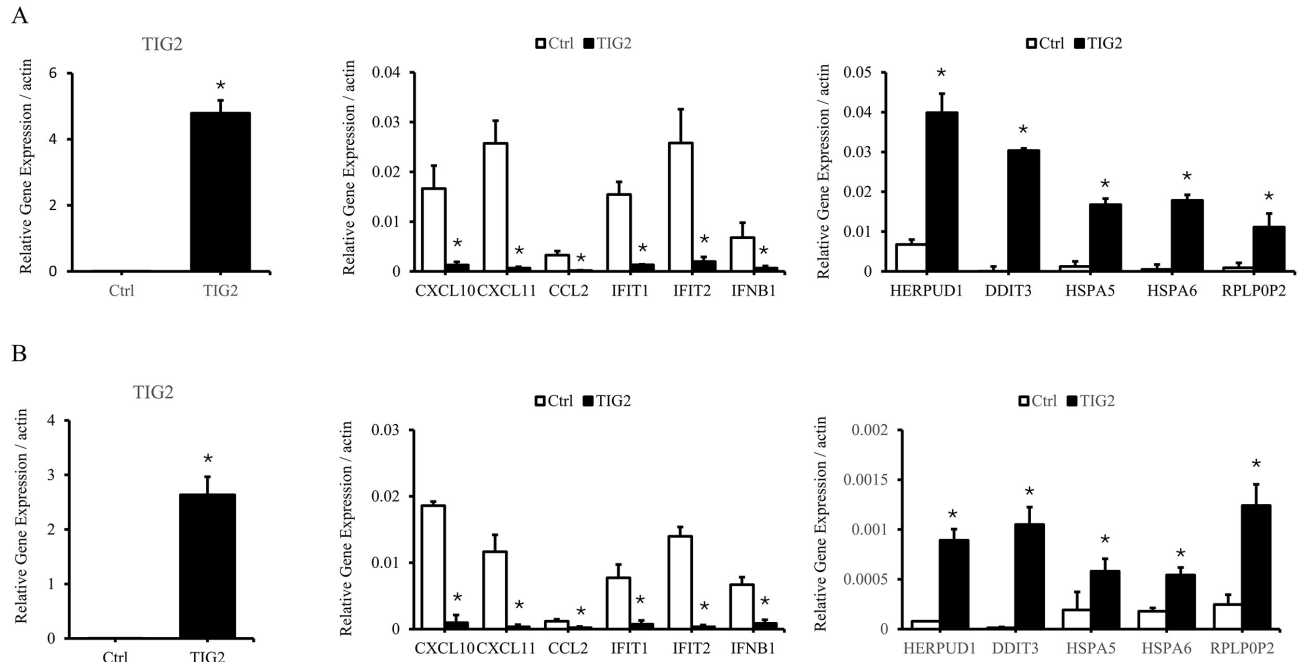


Fig. 5. Validation of TIG2-regulated transcripts in melanoma cells. Following transient expression of TIG2-C-Myc or the empty vector for 24 h, total RNA was isolated from A2058 (A) and A375 (B) cells and analyzed by quantitative real-time PCR. Relative mRNA abundance was normalized to β-actin. Values are presented as the mean ± SD from three independent experiments. *$p < 0.05$ versus control.

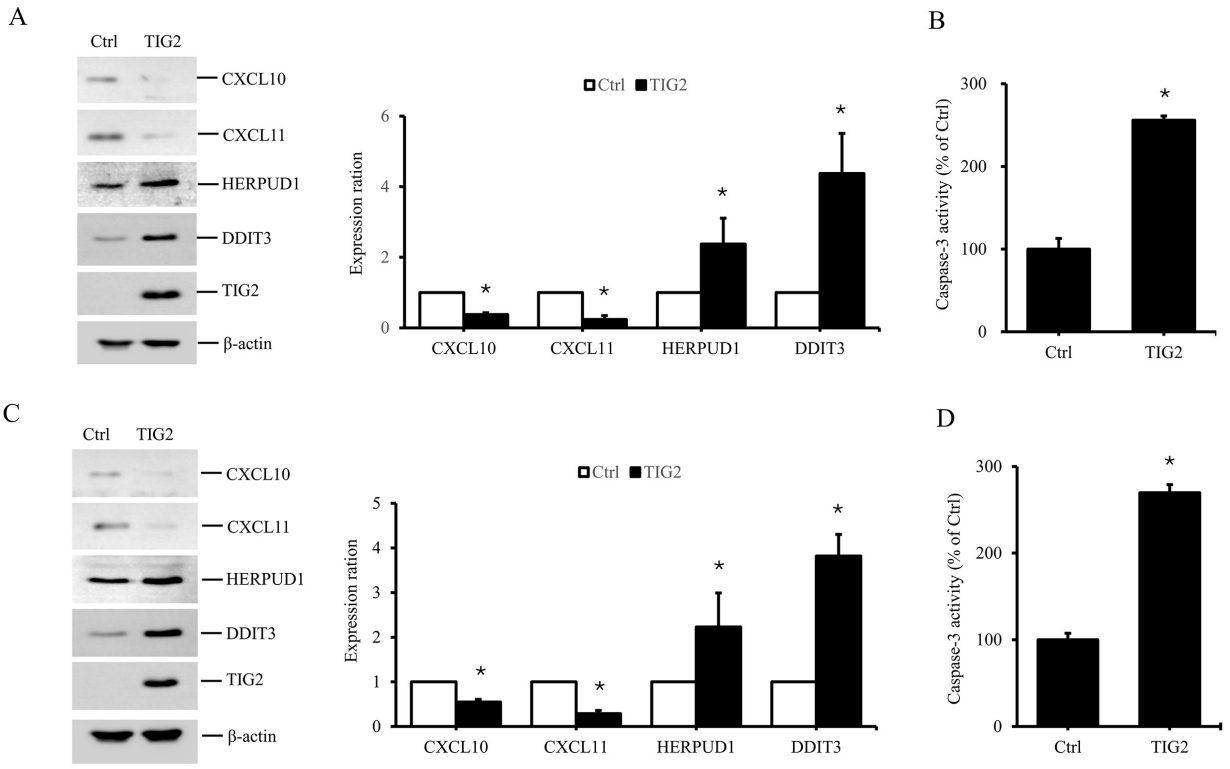


Fig. 6. TIG2 regulates endoplasmic reticulum (ER) stress- and chemokine-associated proteins in melanoma cells. Protein lysates from A2058 (A,B) and A375 (C,D) cells expressing TIG2-C-Myc or the empty vector were analyzed by Western blotting to assess CXCL10, CXCL11, HERPUD1, and DDIT3 protein levels (A,C). Representative immunoblots are shown, together with densitometric quantification from three independent experiments. Caspase-3 enzymatic activity was determined using a colorimetric assay (B,D). *$p < 0.05$ versus control.

(ANOVA), followed by Dunnett's multiple-comparison test when appropriate. For all analyses, a two-tailed p-value < 0.05 was considered statistically significant. Unless otherwise indicated, all graphical data represent results from three independent biological replicates.

3. Results

3.1 TIG2 Expression Is Reduced in Skin Cancer Tissues

To investigate the potential role of *TIG2* in skin carcinogenesis, we analyzed *TIG2* expression in normal skin tissues and skin cancer samples using The Cancer Genome Atlas (TCGA) database. Since TCGA does not contain normal skin tissue data, normal skin samples from healthy donors in the Genotype-Tissue Expression database were used for comparison. Although *TIG2* expression tended to be lower in tumor tissues, no statistically significant difference was observed compared with normal tissues (Fig. 1A). However, further analysis using the OncoDB database demonstrated a clear trend toward reduced *TIG2* expression in skin cancer tissues (Fig. 1B).

In addition to database analyses, we examined *TIG2* expression in a commercially available melanoma tissue array. As shown in Fig. 1C, *TIG2* expression was relatively high in normal skin tissues but markedly decreased in melanoma tissues. We subsequently evaluated the relationship between TIG2 expression and patient survival using the OncoDB database (https://oncodb.org/cgi-bin/survival_gene_profile.cgi). Although patients with high *TIG2* expression (n = 38) had a slightly better 10-year survival rate than those with low *TIG2* expression (n = 37), the difference was not statistically significant (data not shown). Collectively, these findings suggest that TIG2 participates in the early stages of melanoma tumorigenesis, primarily through the regulation of cell growth.

3.2 Ectopic TIG2 Expression Impairs Melanoma Cell Survival

Before performing functional analyses, endogenous TIG2 protein expression was examined in A2058 and A375 melanoma cells by Western blotting. No detectable endogenous TIG2 protein was observed in either cell line under the experimental conditions used (data not shown). Because endogenous TIG2 expression was undetectable, loss-of-function experiments could not be reliably performed in these melanoma cell models. The biological function of TIG2 was therefore investigated using an ectopic overexpression approach throughout this study.

To determine whether TIG2 affects melanoma cell survival, A2058 and A375 cells were transiently transfected with the TIG2-C-Myc expression plasmid. As shown in Fig. 2A, ectopic expression of TIG2 significantly reduced cell viability after 48 h in both melanoma cell lines compared with the empty vector control. We next investigated whether this reduction in cell viability was accompanied by increased cell death. LDH release assays demonstrated that TIG2 significantly increased cytotoxicity in A2058 cells at both 24 and 48 h, whereas a significant increase was observed in A375 cells after 48 h (Fig. 2B). Collectively, these findings indicate that ectopic expression of TIG2 suppresses melanoma cell survival and promotes cell death.

3.3 Identification of TIG2-Regulated Genes in A2058 Cells

Because TIG2 expression was found to inhibit melanoma cell growth, we used RNA-seq to investigate the downstream genes regulated by TIG2 in A2058 cells. MA and volcano plot analyses revealed that most genes did not exhibit significant changes in expression following TIG2 overexpression, with the exception of 32 downregulated genes and 10 upregulated genes (Fig. 3A,B). TIG2 (RARRES2 in Fig. 3B) showed a marked increase in expression (log2 fold change >5), as indicated by the triangle in Fig. 3A.

Fig. 3C presents a heatmap illustrating the differential gene expression patterns between control and TIG2-overexpressing cells. Fig. 4A further summarizes the genes showing significant fold-changes in response to TIG2 expression. Gene Ontology dot plot analysis of these 42 significantly altered genes revealed they were mainly associated with cytokine activation and viral interaction pathways (Fig. 4B), and included *CXCL10*, *CXCL11*, *TNF*, *CSF3*, and *TNFSF10* (Fig. 4C).

The 10 upregulated genes were further analyzed using the g:Profiler database (http://biit.cs.ut.ee/gprofiler/gost) to identify potential signaling pathways associated with TIG2. The most enriched pathways were closely related to ER stress responses (Fig. 4D). TIG2-regulated ER stress-related genes included *DDIT3*, *HYOU1*, *SEL1L*, *HSPA5*, and *HERPUD1*. Similar results were obtained using the Reactome Pathway Database (data not shown). These findings suggest that TIG2 regulates melanoma growth through cytokine modulation and the ER stress response.

3.4 TIG2 Downregulates Chemokine Genes and Upregulates ER Stress-Related Genes

To validate the RNA-seq results, mRNA was collected from A2058 and A375 cells transfected with either an empty vector or a TIG2 expression plasmid, followed by real-time PCR analysis. As shown in Fig. 5A, TIG2 expression was markedly increased in TIG2-transfected cells. In contrast, the expression of cytokines and chemokines, including *CXCL10*, *CXCL11*, and *CCL2*, was significantly downregulated in TIG2-overexpressing cells (Fig. 5A). Conversely, ER stress-related genes, such as *HERPUD1*, *DDIT3*, and several heat shock proteins, were significantly upregulated following TIG2 expression (Fig. 5A). Similar results were observed in A375 cells, where TIG2 expression also reduced cytokine and chemokine expression, while increasing ER stress-related gene expression (Fig. 5B).

In addition to mRNA expression, we analyzed whether TIG2 altered the protein levels of these regulated genes. As shown in Fig. 6A, TIG2 expression in A2058 cells markedly reduced the protein levels of CXCL10 and CXCL11. In contrast, the protein expression levels of HERPUD1 and DDIT3 were significantly increased upon TIG2 overexpression (Fig. 6A). As endogenous CCL2 protein was undetectable in A2058 cells, the effect of TIG2 on CCL2 protein expression could not be determined (data not shown). Similar findings were observed in A375 cells, where TIG2 expression suppressed CXCL10 and CXCL11 protein levels and enhanced HERPUD1 and DDIT3 expression (Fig. 6C). We further examined whether TIG2-induced ER stress was associated with apoptotic signaling by measuring the activity of caspase-3. As shown in Fig. 6B,D, TIG2 overexpression significantly increased caspase-3 activity in both A2058 and A375 cells, supporting the involvement of apoptosis in TIG2-mediated cell death.

Because TIG2 is a secreted protein, we further investigated whether extracellular TIG2 could reproduce the biological effects observed following overexpression of intracellular TIG2. Western blot analysis confirmed that TIG2-Myc protein was readily detected in conditioned media collected from TIG2-transfected A2058 and A375 cells (**Supplementary Fig. 1A**). However, culturing naïve A2058 or A375 cells in TIG2-containing conditioned medium did not significantly alter the protein expression of CXCL10, CXCL11, HERPUD1, or DDIT3 (**Supplementary Fig. 1B,C**). Likewise, neither cell viability nor LDH release was significantly affected under these conditions (**Supplementary Fig. 1D,E**). These findings suggest that conditioned medium containing secreted TIG2 was insufficient to reproduce the intracellular responses induced by TIG2 overexpression, indicating the observed biological effects are more likely to be mediated through intracellular mechanisms rather than an autocrine action of secreted TIG2.

3.5 Effects of CXCL10 and CXCL11 on TIG2-Mediated Regulation of Cell Growth

CXCL10 and CXCL11 regulate the chemotaxis of immune cells (e.g., T cells, NK cells, and macrophages) via the CXCR3 receptor [29]. CXCL10 promotes the activation of proangiogenic and pro-growth signaling molecules in murine B16F10 melanoma cells, thereby enhancing cell proliferation [30]. CXCL10 has also been described as an oncogenic factor involved in cancer metastasis [31]. Although studies on CXCL11 in melanoma are limited, several reports have suggested that elevated serum CXCL11

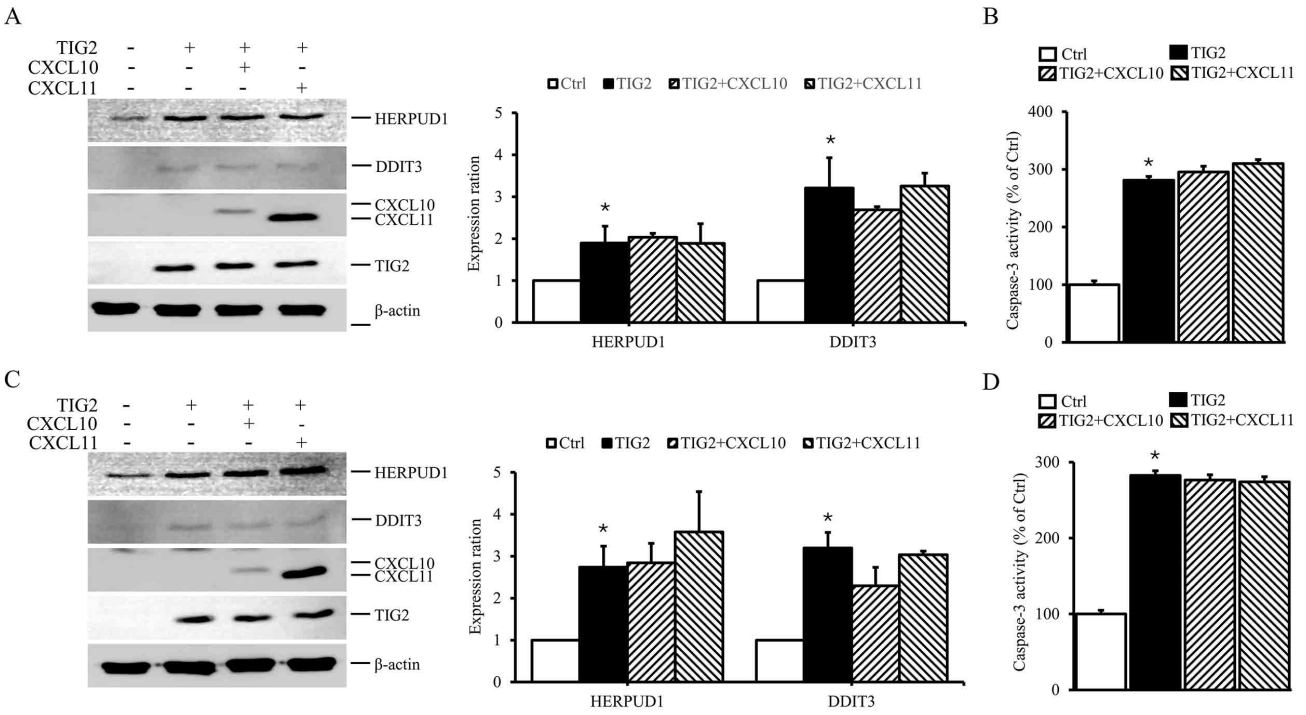


Fig. 7. Restoration of CXCL10 or CXCL11 does not alter TIG2-induced ER stress signaling. A2058 (A,B) and A375 (C,D) cells were transfected with empty vector, TIG2-C-Myc alone, or TIG2-C-Myc together with CXCL10-Flag or CXCL11-Flag expression plasmids. HERPUD1 and DDIT3 protein expression was examined by Western blotting after 24 h (A,C). Representative blots and quantitative analyses are shown. Caspase-3 activity was measured in parallel (B,D). *$p < 0.05$ versus control.

levels in patients receiving immune checkpoint inhibitors are associated with poor survival outcomes, implying a potential oncogenic role [32].

Because TIG2 expression downregulated CXCL10 and CXCL11, we next investigated whether exogenous supplementation with CXCL10 or CXCL11 could rescue the effects of TIG2 on cell growth. As shown in Fig. 7A, co-treatment of A2058 cells with TIG2 and either CXCL10 or CXCL11 did not alter expression of the ER stress-related proteins HERPUD1 and DDIT3. Similar results were observed in A375 cells, which showed that CXCL10 and CXCL11 treatment did not alter TIG2-induced upregulation of HERPUD1 and DDIT3 (Fig. 7C).

Next, we evaluated caspase-3 activity to determine whether these chemokines could modulate TIG2-induced apoptotic signaling. As shown in Fig. 7B,D, TIG2 overexpression significantly increased caspase-3 activity in both A2058 and A375 cells. However, exogenous CXCL10 or CXCL11 failed to reverse this effect, indicating that TIG2-induced activation of apoptotic signaling is independent of CXCL10/CXCL11-mediated pathways.

We further examined whether CXCL10 or CXCL11 could attenuate the TIG2-induced reduction in cell viability and increase in cell death. As shown in Fig. 8, neither CXCL10 nor CXCL11 significantly affected the TIG2-mediated suppression of cell viability (Fig. 8A) or induction of cell death (Fig. 8B). The results suggest that although TIG2 can downregulate CXCL10 and CXCL11 expression, these chemokines are not the major mediators responsible for TIG2-induced growth suppression.

3.6 TUDCA Attenuates TIG2-Induced ER Stress Responses and Reverses TIG2-Mediated Growth Suppression

In addition to suppressing the expression of CXCL10 and CXCL11, TIG2 also enhanced the expression of ER stress-related proteins. Therefore, we used the chemical chaperone TUDCA, an inhibitor of ER stress responses [33,34], to investigate the importance of ER stress signaling in TIG2-mediated growth regulation.

As shown in Fig. 9A, TUDCA treatment effectively prevented the TIG2-induced upregulation of HERPUD1 and DDIT3 in A2058 cells. However, TUDCA did not affect the TIG2-mediated downregulation of CXCL10 and CXCL11 protein expression. Similar findings were observed in A375 cells, where TUDCA suppressed TIG2-induced HERPUD1 and DDIT3 expression but did not alter CXCL10 or CXCL11 levels (Fig. 9C).

Next, we examined caspase-3 activity to determine whether ER stress modulation also impacted TIG2-induced apoptotic signaling. As shown in Fig. 9B,D, TIG2 overexpression significantly increased caspase-3 activity in both A2058 and A375 cells. Importantly, TUDCA treatment partially reversed this effect, reducing caspase-3 activity in TIG2-expressing cells. These findings indicate that TIG2-

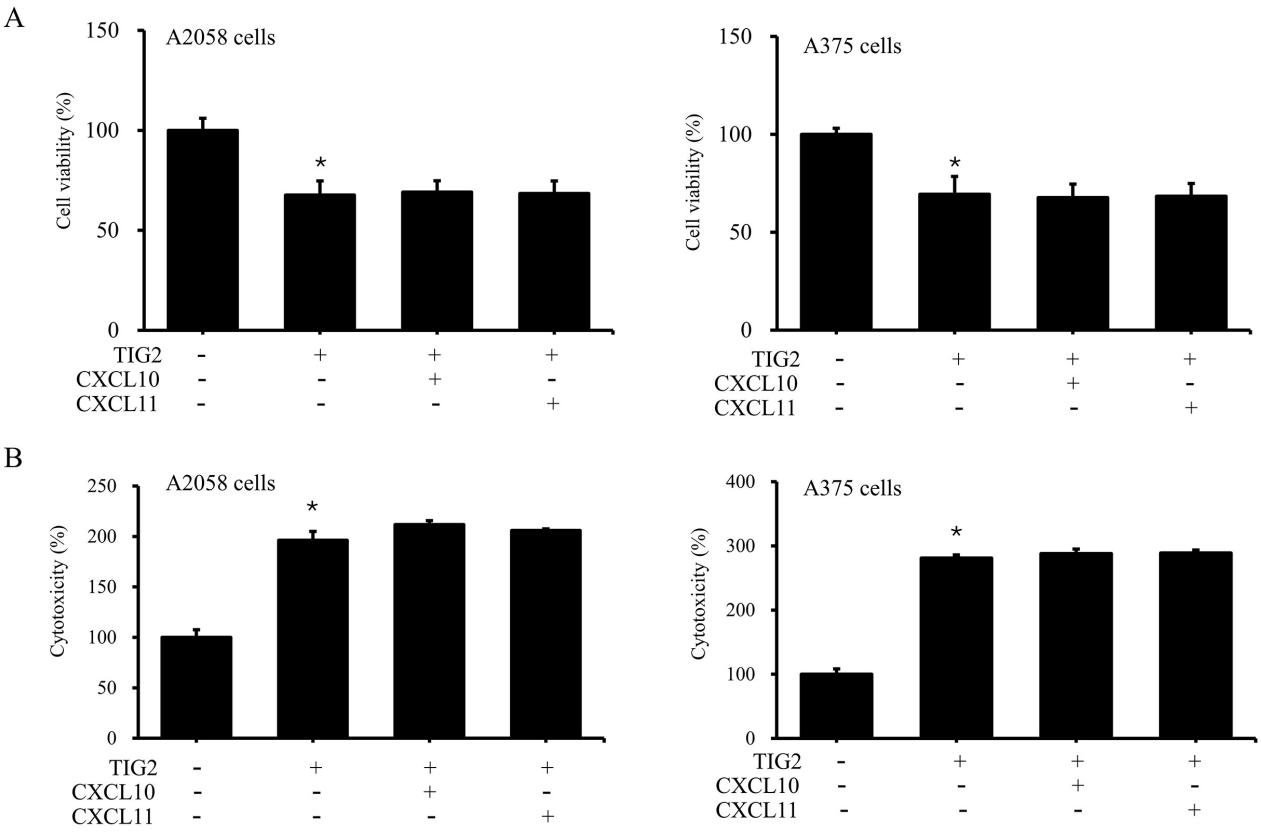


Fig. 8. Overexpression of CXCL10 or CXCL11 fails to rescue TIG2-induced cytotoxicity. Melanoma cells were transfected with the indicated expression vectors and cultured for 48 h. Cell viability was assessed by the WST-1 assay (A), whereas LDH release was used to evaluate cytotoxicity (B). Results are expressed as the mean ± SD of three independent experiments. *$p < 0.05$ versus control.

induced ER stress contributes functionally to the activation of apoptotic pathways, and that pharmacological attenuation of ER stress can partially rescue TIG2-mediated cytotoxicity.

We examined whether TUDCA could attenuate the effects of TIG2 on cell growth. As shown in Fig. 10, TUDCA reduced TIG2-induced HERPUD1 and DDIT3 expression in both A2058 and A375 cells. Moreover, it significantly rescued the TIG2-mediated reductions in cell viability (Fig. 10A) and TIG2-induced cell death (Fig. 10B). Collectively, these results suggest that TIG2 suppresses melanoma cell viability and promotes cell death primarily through activation of the ER stress response pathway.

4. Discussion

This study found that TIG2 expression is reduced in both skin cancer tissues and melanoma cell lines, whereas its overexpression significantly suppresses cell viability and induces cell death. RNA-seq analysis combined with experimental validation revealed that TIG2 downregulates multiple chemokines, including *CXCL10*, *CXCL11*, and *CCL2*, while simultaneously upregulating ER stress-related genes such as *HERPUD1* and *DDIT3*. Although TIG2 expression was consistently reduced in melanoma tissues and its ectopic expression inhibited the growth of melanoma cells, the survival analysis based on public databases did not reach statistical significance. Therefore, the present findings support a tumor-suppressive role for TIG2 in melanoma cells rather than establishing it as a definitive tumor suppressor gene in clinical melanoma. Additional studies using larger patient cohorts and *in vivo* tumor models will be required to further determine the prognostic and therapeutic significance of TIG2 in melanoma.

Among the chemokines regulated by TIG2, CCL2 has been reported to promote tumor growth and suppress immune cell activity [35]. Elevated circulating levels of CCL2 have also been observed in patients with metastatic melanoma [36], and its expression has been linked to microRNA regulation (miR-34a, miR-100, and miR-125b) and drug resistance [37]. However, because we were unable to detect CCL2 in our experimental system, its precise role in TIG2-mediated regulation remains unclear.

In contrast, although reported to possess tumor-promoting potential in certain contexts, CXCL10 and CXCL11 primarily recruit CXCR3-expressing immune cells, including NK and T cells. Previous studies have shown that TIG2 can recruit CMKLR1-expressing NK cells into the tumor microenvironment, thereby enhancing an-

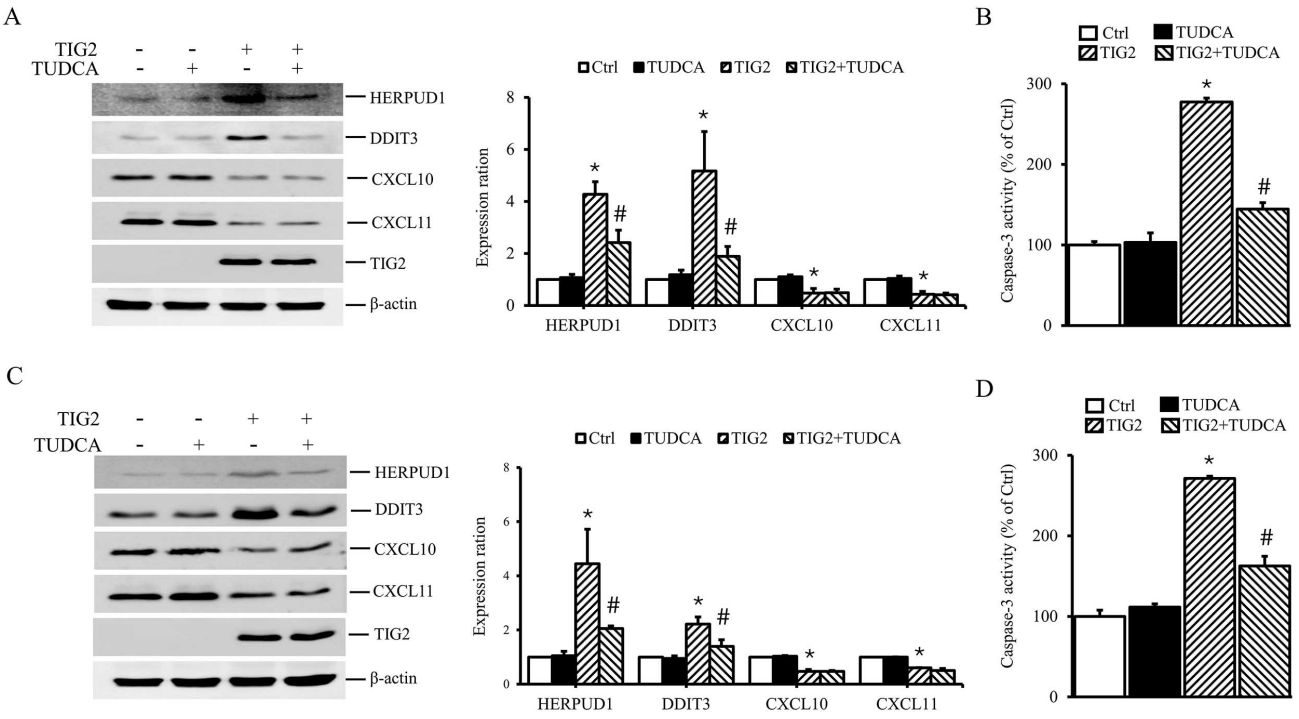


Fig. 9. TUDCA attenuates TIG2-induced ER stress signaling. A2058 (A,B) and A375 (C,D) cells expressing TIG2-C-Myc or the empty vector were treated with 500 μM TUDCA for 24 h. Protein expression of HERPUD1, DDIT3, CXCL10, and CXCL11 was analyzed by Western blotting (A,C). Representative blots and quantitative analyses are shown. Caspase-3 activity was measured in parallel (B,D). *$p < 0.05$ versus control; $^{\#}p < 0.05$ versus TIG2 alone. TUDCA, tauroursodeoxycholic acid.

titumor immunity in several experimental models [8]. In contrast, our data demonstrate that TIG2 overexpression suppresses CXCL10 and CXCL11 expression in melanoma cells. CXCL10 and CXCL11 are important chemoattractants for CXCR3-positive immune cells, including NK cells and activated T lymphocytes. Therefore, our findings suggest that TIG2 may regulate immune-cell recruitment through multiple, and potentially distinct, signaling mechanisms. However, because the present study did not include immune-cell co-culture experiments, migration assays, or *in vivo* immune analyses, the immunological consequences of these chemokine changes remain speculative and require further investigation.

Because TIG2 is a secreted protein, we further examined whether extracellular TIG2 could reproduce the biological effects observed following intracellular TIG2 overexpression. However, conditioned medium collected from TIG2-overexpressing melanoma cells failed to alter ER stress-associated proteins, chemokine expression, cell viability, or cell death in recipient melanoma cells (**Supplementary Fig. 1**). These findings suggest the biological effects observed in the present study are unlikely to result from an autocrine action of secreted TIG2. Our observations are also consistent with transcriptomic data showing that A2058 and A375 cells express little or no detectable CMKLR1 (https://www.proteinatlas.org/ENSG00000174600-CMKLR1/cell+line), the major functional receptor for TIG2. Therefore, the ER stress activation and growth inhibition observed in this study most likely reflect intracellular functions of ectopically expressed TIG2 rather than receptor-mediated extracellular signaling.

Collectively, members of the tazarotene-induced gene family (TIG1–TIG3) exhibit multilayered tumor-suppressive mechanisms in melanoma. TIG1 inhibits melanoma progression through the VAC14 component of the PIKFYVE complex/mammalian target of rapamycin pathway and ER stress induction [25,26]. It also suppresses tumor growth via Schlafen 11 [38]. TIG3 induces apoptosis by downregulating inhibitors of apoptosis proteins and activating caspase-3 [27], while TIG2 appears to regulate both ER stress responses and tumor immune modulation. Although protein overexpression generally can induce ER stress [39,40], TIG3 overexpression does not. This suggests that ER stress induction by TIG1 and TIG2 represents a specific regulatory response rather than a consequence of nonspecific protein accumulation.

Therefore, the anti-melanoma effects of tazarotene may result from the coordinated actions of TIG1 and TIG3 through multiple pathways, including intracellular stress responses, signaling regulation, and immune cell recruitment, providing important insights for future therapeutic strategies.

ER stress is increasingly recognized as a context-dependent process during cancer progression. Its contribu-

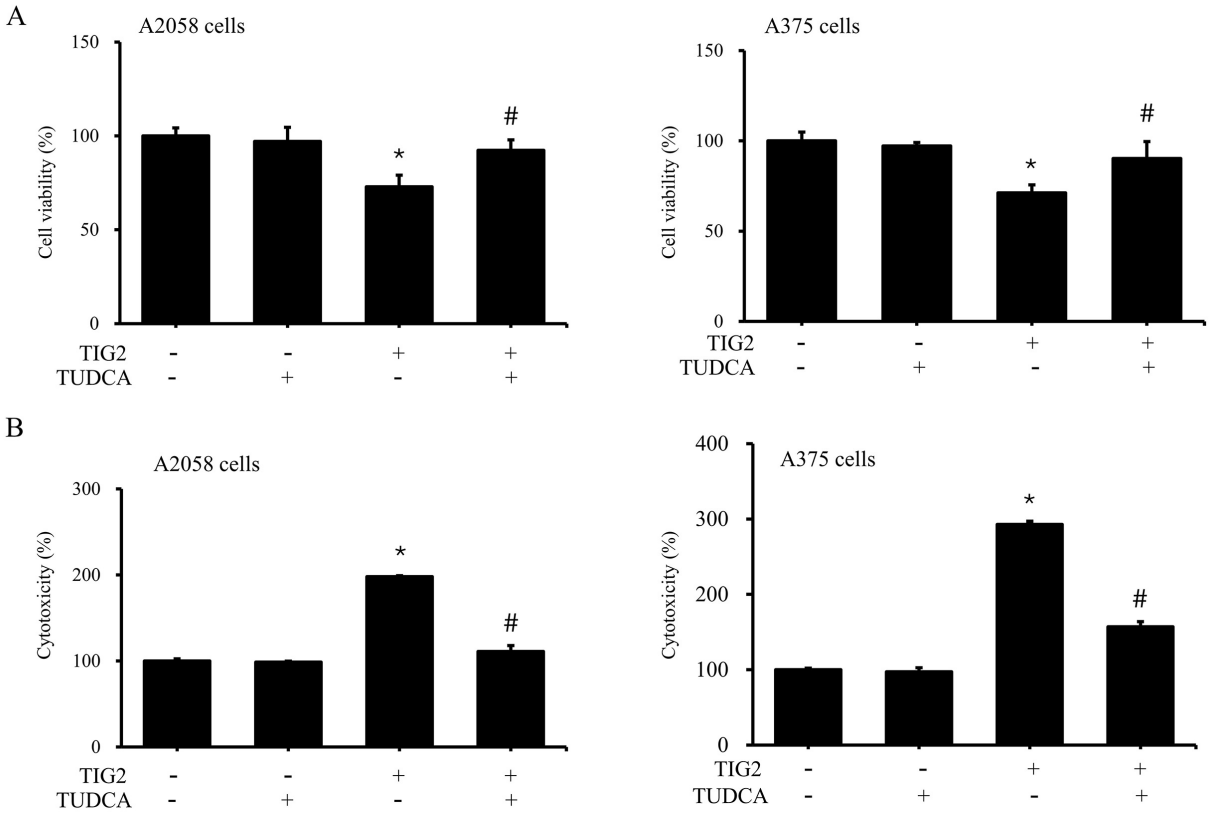


Fig. 10. Pharmacological inhibition of ER stress partially rescues TIG2-induced loss of cell viability. Following transfection with TIG2-C-Myc or the empty vector, A2058 and A375 cells were incubated in the presence or absence of 500 μM TUDCA for 48 h. Cell viability was then determined using the WST-1 assay (A), and LDH release was used to evaluate cytotoxicity (B). Data are expressed as the mean ± SD of three independent experiments. *$p < 0.05$ versus control; $^{\#}p < 0.05$ versus TIG2 alone.

tion to tumor cell survival or cell death appears to depend on the magnitude and duration of the unfolded protein response (UPR) [41,42]. Tumor cells are continuously exposed to hypoxia, nutrient deprivation, oxidative stress, and elevated protein synthesis, resulting in persistent ER stress and activation of the UPR. Initially, activation of the UPR serves as an adaptive mechanism that restores ER homeostasis by reducing protein synthesis and enhancing protein-folding capacity. However, when ER stress is prolonged or exceeds the adaptive capacity of the UPR, the three canonical ER stress sensors—protein kinase R-like endoplasmic reticulum kinase (PERK), inositol-requiring enzyme 1α (IRE1α), and activating transcription factor 6 (ATF6)—shift signaling from pro-survival to pro-death pathways, ultimately triggering apoptosis or other forms of regulated cell death [43].

Recent studies have demonstrated that adaptive UPR signaling contributes to melanoma progression, metastatic potential, and resistance to targeted therapies [44]. Conversely, sustained activation of ER stress has also been reported to suppress melanoma growth by inducing apoptosis, autophagy-associated cell death, or immunogenic cell death [45,46]. In particular, activation of the PERK–eIF2α–ATF4–CHOP signaling axis has been implicated in melanoma cell responses to oxidative stress, hypoxia, and anticancer treatments, while excessive CHOP/DDIT3 activation is generally associated with irreversible ER stress and apoptosis [46,47].

In the present study, TIG2 overexpression consistently increased the expression of HERPUD1 and DDIT3, and pharmacological attenuation of ER stress with TUDCA partially rescued TIG2-induced growth inhibition and cell death. These findings support the involvement of ER stress in the biological effects of TIG2. However, because only selected ER stress-associated markers were examined, the present study was unable to determine which of the canonical UPR branches (PERK, IRE1α, or ATF6) is primarily responsible for TIG2-mediated signaling. Further investigation of these upstream UPR pathways will be required to define the precise molecular mechanism underlying TIG2-induced ER stress.

The current study found that TIG2 markedly upregulated HERPUD1 and DDIT3 expression. Furthermore, TUDCA partially reversed TIG2-induced cytotoxicity, supporting the notion that TIG2-mediated ER stress is not merely a secondary phenomenon but a key mechanism underlying its tumor-suppressive effects. HERPUD1 is a critical regulator of the ER-associated degradation system and

is involved in clearing misfolded proteins and maintaining ER homeostasis [48], whereas DDIT3/CHOP is a central transcription factor that drives apoptosis under prolonged ER stress conditions [46,49,50]. Thus, TIG2 may impair protein quality control, ER folding capacity, or redox balance, thereby activating downstream stress pathways such as PERK–CHOP and ultimately reducing melanoma cell survival.

Emerging evidence further indicates that cellular stress responses may influence tumor immune recognition independently of their direct cytotoxic effects. Several recent studies have demonstrated that pharmacological induction of ER stress or integrated stress responses can enhance melanoma susceptibility to NK-cell-mediated cytotoxicity by increasing the expression of activating NK-cell ligands, including ULBP1 and other NKG2D ligands [51,52,53]. These findings suggest that stress-response pathways may simultaneously regulate melanoma cell survival and immune visibility, thereby contributing to antitumor immunity beyond the direct induction of cell death. Moreover, ER stress is increasingly being recognized as an important regulator of the tumor immune microenvironment. Excessive ER stress can alter cytokine and chemokine secretion and disrupt antigen presentation, immune cell activation, and immune evasion mechanisms [46]. Therefore, TIG2-mediated regulation of CXCL10 and CXCL11 may reflect a broader association between ER stress and immune signaling in melanoma. Because ER stress has been implicated in regulating cytokine secretion, antigen presentation, and NK-cell activation, it is conceivable that TIG2-induced ER stress could indirectly influence the tumor immune microenvironment. Nevertheless, the present study did not directly examine immune cell recruitment and infiltration, or NK-cell cytotoxicity. Consequently, these immunological implications should be considered hypothesis-generating rather than definitive conclusions [54,55]. Future studies that integrate melanoma–immune cell co-culture systems, NK-cell migration assays, and immunocompetent animal models will be necessary to determine whether TIG2-mediated ER stress enhances immune recognition through modulation of chemokine expression or activation of stress-induced NK-cell ligands.

5. Limitations

Several limitations of this study should be acknowledged. First, all functional experiments were performed using cultured melanoma cell lines; therefore, the effects of TIG2 on the tumor immune microenvironment could not be directly evaluated. Second, although TUDCA experiments support the involvement of ER stress, only selected ER stress-associated markers were examined. Comprehensive characterization of the canonical UPR branches, including PERK, IRE1α, and ATF6 signaling, is required in future studies.

Third, the biological function of TIG2 was investigated primarily using a gain-of-function approach. Loss-of-function experiments could not be reliably performed in these models because endogenous TIG2 expression was undetectable in both A2058 and A375 melanoma cells. Future studies employing melanoma models with detectable endogenous TIG2 expression will be necessary to further validate its physiological functions.

Finally, TIG2 is a secreted protein that primarily exerts its biological activities through receptors such as CMKLR1. Publicly available transcriptomic datasets indicate that A2058 and A375 cells express little or no detectable CMKLR1, suggesting that an autocrine chemerin–CMKLR1 signaling loop is unlikely to operate in these cell lines. Consequently, the present study mainly reflects the intracellular consequences associated with TIG2 overexpression rather than receptor-mediated extracellular signaling. Further studies using CMKLR1-positive melanoma models or co-culture systems will be required to clarify the contribution of extracellular TIG2 signaling to melanoma progression.

6. Conclusions

This study demonstrates for the first time that *TIG2* is downregulated in skin cancer tissues and melanoma cells, and that its overexpression significantly inhibits melanoma cell viability and induces cell death. RNA-seq and molecular analyses demonstrated that TIG2 regulates multiple chemokines associated with tumor progression and modulation of the immune microenvironment, including CXCL10, CXCL11, and CCL2, while concurrently activating ER stress-related genes such as *HERPUD1* and *DDIT3*. Furthermore, the chemical chaperone TUDCA partially rescues TIG2-induced cytotoxic effects, supporting the notion that the anti-proliferative effects of TIG2 are closely associated with ER stress activation.

Although exogenous CXCL10 and CXCL11 failed to reverse the effects of TIG2, their regulation suggested that TIG2 may participate in shaping the tumor immune microenvironment. Collectively, our findings suggest that TIG2 exerts tumor-suppressive effects in melanoma and may represent an important molecular link between ER stress, cell survival, and immune regulation.

Abbreviations

ATF, activating transcription factor; BCA, bicinchoninic acid; BRAF, B-Raf proto-oncogene, serine/threonine kinase; CCL2, chemokine (C-C motif) ligand 2; CHOP, C/EBP homologous protein; CMKLR1, chemokine-like receptor 1; CXCL, C-X-C motif chemokine ligand; DDIT3, DNA damage-inducible transcript 3; EIA, enzyme immuno assay; ER, endoplasmic reticulum; FBS, fetal bovine serum; FPKM, Fragments Per Kilobase of transcript per Million mapped reads; GO, Gene Ontology; HERPUD1, homocysteine inducible ER protein

with ubiquitin-like domain 1; IRE1α, inositol-Requiring Enzyme 1α; LDH, lactate dehydrogenase; NK, natural killer; PERK, PKR-like endoplasmic reticulum kinase; RARRES2, retinoic acid receptor responder 2; RNA-seq, RNA sequencing; SD, standard deviation; STR, short tandem repeat; TCGA, The Cancer Genome Atlas; TIG2, Tazarotene-induced gene 2; TIGs, tazarotene-induced genes; TUDCA, tauroursodeoxycholic acid; UPR, unfolded protein response.

Availability of Data and Materials

All data generated or analyzed during this study are included in the article, further inquiries can be directed to the corresponding author.

Author Contributions

CHW and FMT designed the research study. CHW and LKW performed the research. LKW and FMT analyzed the data. CHW and FMT wrote the manuscript. All authors contributed to editorial changes in the manuscript. All authors read and approved the final manuscript. All authors have participated sufficiently in the work and agreed to be accountable for all aspects of the work.

Ethics Approval and Consent to Participate

The study was carried out in accordance with the guidelines of the Declaration of Helsinki. The requirement for ethical approval and informed consent was waived by the Taipei Tzu Chi Hospital, Buddhist Tzu Chi Medical Foundation Institutional Review Board because the study used commercially available, de-identified human tissue cDNA samples and did not involve direct recruitment of participants, collection of human tissue, or access to identifiable patient information.

Acknowledgment

The authors thank the Core Laboratory of Taipei Tzu Chi Hospital for support. The graphical abstract was created in BioRender. The manuscript underwent professional English-language editing by YodaEdit.

Funding

This study was supported by grants from the Taipei Tzu Chi Hospital through grants from the Buddhist Tzu Chi Medical Foundation (Research project numbers: TCRD-TPE-113-20 and TCRD-TPE-114-21).

Conflicts of Interest

The authors declare no conflicts of interest. Fu-Ming Tsai is serving as one of the Guest editors of this journal. We declare that Fu-Ming Tsai had no involvement in the peer review of this article and has no access to information regarding its peer review. Full responsibility for the editorial process for this article was delegated to Amancio Carnero Moya. This research was funded by the Buddhist Tzu Chi Medical Foundation, the institution where several authors are affiliated. The authors declare that the funder had no role in the design of the study; in the collection, analyses, or interpretation of data; in the writing of the manuscript; or in the decision to publish the results.

Declaration of AI and AI-Assisted Technologies in the Writing Process

During the preparation of this manuscript, the authors first used ChatGPT-3.5 solely to improve grammar, spelling, and language clarity. After using these tools and services, the authors carefully reviewed and revised the manuscript as necessary and take full responsibility for the content and the final published version of the manuscript.

Supplementary Material

Supplementary material associated with this article can be found, in the online version, at https://doi.org/10.31083/FBL54095.

References

[1] Nagpal S, Patel S, Jacobe H, DiSepio D, Ghosn C, Malhotra M, et al. Tazarotene-induced gene 2 (TIG2), a novel retinoid-responsive gene in skin. The Journal of Investigative Dermatology. 1997; 109: 91–95. https://doi.org/10.1111/1523-1747.ep12276660

[2] Wittamer V, Franssen JD, Vulcano M, Mirjolet JF, Le Poul E, Migeotte I, et al. Specific recruitment of antigen-presenting cells by chemerin, a novel processed ligand from human inflammatory fluids. The Journal of Experimental Medicine. 2003; 198: 977–985. https://doi.org/10.1084/jem.20030382

[3] Zabel BA, Allen SJ, Kulig P, Allen JA, Cichy J, Handel TM, et al. Chemerin activation by serine proteases of the coagulation, fibrinolytic, and inflammatory cascades. The Journal of Biological Chemistry. 2005; 280: 34661–34666. https://doi.org/10.1074/jbc.M504868200

[4] Bozaoglu K, Bolton K, McMillan J, Zimmet P, Jowett J, Collier G, et al. Chemerin is a novel adipokine associated with obesity and metabolic syndrome. Endocrinology. 2007; 148: 4687–4694. https://doi.org/10.1210/en.2007-0175

[5] Goralski KB, McCarthy TC, Hanniman EA, Zabel BA, Butcher EC, Parlee SD, et al. Chemerin, a novel adipokine that regulates adipogenesis and adipocyte metabolism. The Journal of Biological Chemistry. 2007; 282: 28175–28188. https://doi.org/10.1074/jbc.M700793200

[6] Zabel BA, Zuniga L, Ohyama T, Allen SJ, Cichy J, Handel TM, et al. Chemoattractants, extracellular proteases, and the integrated host defense response. Experimental Hematology. 2006; 34: 1021–1032. https://doi.org/10.1016/j.exphem.2006.05.003

[7] Pachynski RK, Wang P, Salazar N, Zheng Y, Nease L, Rosalez J, et al. Chemerin Suppresses Breast Cancer Growth by Recruiting Immune Effector Cells Into the Tumor Microenvironment. Frontiers in Immunology. 2019; 10: 983. https://doi.org/10.3389/fimmu.2019.00983

[8] Pachynski RK, Zabel BA, Kohrt HE, Tejeda NM, Monnier J, Swanson CD, et al. The chemoattractant chemerin suppresses melanoma by recruiting natural killer cell antitumor defenses. The Journal of Experimental Medicine. 2012; 209: 1427–1435. https://doi.org/10.1084/jem.20112124

[9] Li JJ, Yin HK, Guan DX, Zhao JS, Feng YX, Deng

YZ, et al. Chemerin suppresses hepatocellular carcinoma metastasis through CMKLR1-PTEN-Akt axis. British Journal of Cancer. 2018; 118: 1337–1348. https://doi.org/10.1038/s41416-018-0077-y

[10] Kumar JD, Aolymat I, Tiszlavicz L, Reisz Z, Garalla HM, Beynon R, et al. Chemerin acts via CMKLR1 and GPR1 to stimulate migration and invasion of gastric cancer cells: putative role of decreased TIMP-1 and TIMP-2. Oncotarget. 2019; 10: 98–112. https://doi.org/10.18632/oncotarget.26414

[11] Cai Q, Huang Z, Qi L, Wang T, Shen Y, Huang J. Tazarotene-induced gene 2 is associated with poor survival in non-small cell lung cancer. Oncology Letters. 2016; 12: 2680–2685. https://doi.org/10.3892/ol.2016.5025

[12] Miller AJ, Mihm MC, Jr. Melanoma. The New England Journal of Medicine. 2006; 355: 51–65. https://doi.org/10.1056/NEJMra052166

[13] Caraviello C, Nazzaro G, Tavoletti G, Boggio F, Denaro N, Murgia G, et al. Melanoma Skin Cancer: A Comprehensive Review of Current Knowledge. Cancers. 2025; 17: 2920. https://doi.org/10.3390/cancers17172920

[14] Druskovich C, Kelley J, Aubrey J, Palladino L, Wright GP. A Review of Melanoma Subtypes: Genetic and Treatment Considerations. Journal of Surgical Oncology. 2025; 131: 356–364. https://doi.org/10.1002/jso.27953

[15] Schadendorf D, Fisher DE, Garbe C, Gershenwald JE, Grob JJ, Halpern A, et al. Melanoma. Nature Reviews. Disease Primers. 2015; 1: 15003. https://doi.org/10.1038/nrdp.2015.3

[16] Davies H, Bignell GR, Cox C, Stephens P, Edkins S, Clegg S, et al. Mutations of the BRAF gene in human cancer. Nature. 2002; 417: 949–954. https://doi.org/10.1038/nature00766

[17] Florent L, Saby C, Slimano F, Morjani H. BRAF V600-Mutated Metastatic Melanoma and Targeted Therapy Resistance: An Update of the Current Knowledge. Cancers. 2023; 15: 2607. https://doi.org/10.3390/cancers15092607

[18] Menzer C, Dugas-Breit S, Dugas M, Blank CU, Groen EJ, Reijers I, et al. Targeted therapy for rare BRAF-mutated melanoma: Updated multicenter analysis and launch of a publicly accessible online outcome database. European Journal of Cancer (Oxford, England: 1990). 2025; 228: 115703. https://doi.org/10.1016/j.ejca.2025.115703

[19] Liang Y, Zheng Y, Zeng Y, Hu C, Si Y, Fan X, et al. Immune checkpoint inhibitors in melanoma: mechanisms, immune cell interactions, and the tumour microenvironment. Frontiers in Immunology. 2025; 16: 1691608. https://doi.org/10.3389/fimmu.2025.1691608

[20] Pham JP, Staeger R, Joshua AM, Liu J, da Silva IP, Dummer R, et al. An updated review of immune checkpoint inhibitors in cutaneous oncology: Beyond melanoma. European Journal of Cancer (Oxford, England: 1990). 2025; 214: 115121. https://doi.org/10.1016/j.ejca.2024.115121

[21] Altucci L, Gronemeyer H. The promise of retinoids to fight against cancer. Nature Reviews. Cancer. 2001; 1: 181–193. https://doi.org/10.1038/35106036

[22] Bianchi L, Orlandi A, Campione E, Angeloni C, Costanzo A, Spagnoli LG, et al. Topical treatment of basal cell carcinoma with tazarotene: a clinicopathological study on a large series of cases. The British Journal of Dermatology. 2004; 151: 148–156. https://doi.org/10.1111/j.1365-2133.2004.06044.x

[23] Tang XH, Gudas LJ. Retinoids, retinoic acid receptors, and cancer. Annual Review of Pathology. 2011; 6: 345–364. https://doi.org/10.1146/annurev-pathol-011110-130303

[24] Nagpal S, Patel S, Asano AT, Johnson AT, Duvic M, Chandraratna RA. Tazarotene-induced gene 1 (TIG1), a novel retinoic acid receptor-responsive gene in skin. The Journal of Investigative Dermatology. 1996; 106: 269–274. https://doi.org/10.1111/1523-1747.ep12340668

[25] Wang CH, Wang LK, Wu CC, Chen ML, Kuo CY, Shyu RY, et al. TIG1 Inhibits the mTOR Signaling Pathway in Malignant Melanoma Through the VAC14 Protein. Anticancer Research. 2023; 43: 2635–2643. https://doi.org/10.21873/anticanres.16430

[26] Wang CH, Tzeng IS, Wang LK, Wu CC, Chen ML, Kuo CY, et al. Tazarotene-induced Gene 1 Induces Melanoma Cell Death by Triggering Endoplasmic Reticulum Stress Response. Frontiers in Bioscience (Landmark Edition). 2024; 29: 233. https://doi.org/10.31083/j.fbl2906233

[27] Wang CH, Wang LK, Tsai FM. Tazarotene-Induced Gene 3 (TIG3) Induces Apoptosis in Melanoma Cells Through the Modulation of Inhibitors of Apoptosis Proteins. Biomedicines. 2025; 13: 1749. https://doi.org/10.3390/biomedicines13071749

[28] Wang CH, Lu TJ, Wang LK, Wu CC, Chen ML, Kuo CY, et al. Tazarotene-induced gene 1 interacts with Polo-like kinase 2 and inhibits cell proliferation in HCT116 colorectal cancer cells. Cell Biology International. 2021; 45: 2347–2356. https://doi.org/10.1002/cbin.11681

[29] Tokunaga R, Zhang W, Naseem M, Puccini A, Berger MD, Soni S, et al. CXCL9, CXCL10, CXCL11/CXCR3 axis for immune activation - A target for novel cancer therapy. Cancer Treatment Reviews. 2018; 63: 40–47. https://doi.org/10.1016/j.ctrv.2017.11.007

[30] Kim B, Park YY, Lee JH. CXCL10 promotes melanoma angiogenesis and tumor growth. Animal Cells and Systems. 2024; 28: 453–465. https://doi.org/10.1080/19768354.2024.2402024

[31] Wightman SC, Uppal A, Pitroda SP, Ganai S, Burnette B, Stack M, et al. Oncogenic CXCL10 signalling drives metastasis development and poor clinical outcome. British Journal of Cancer. 2015; 113: 327–335. https://doi.org/10.1038/bjc.2015.193

[32] Koguchi Y, Hoen HM, Bambina SA, Rynning MD, Fuerstenberg RK, Curti BD, et al. Serum Immunoregulatory Proteins as Predictors of Overall Survival of Metastatic Melanoma Patients Treated with Ipilimumab. Cancer Research. 2015; 75: 5084–5092. https://doi.org/10.1158/0008-5472.CAN-15-2303

[33] Lee YY, Hong SH, Lee YJ, Chung SS, Jung HS, Park SG, et al. Tauroursodeoxycholate (TUDCA), chemical chaperone, enhances function of islets by reducing ER stress. Biochemical and Biophysical Research Communications. 2010; 397: 735–739. https://doi.org/10.1016/j.bbrc.2010.06.022

[34] Yoon YM, Lee JH, Yun SP, Han YS, Yun CW, Lee HJ, et al. Tauroursodeoxycholic acid reduces ER stress by regulating of Akt-dependent cellular prion protein. Scientific Reports. 2016; 6: 39838. https://doi.org/10.1038/srep39838

[35] Kadomoto S, Izumi K, Mizokami A. Roles of CCL2-CCR2 Axis in the Tumor Microenvironment. International Journal of Molecular Sciences. 2021; 22: 8530. https://doi.org/10.3390/ijms22168530

[36] Basson C, Serem JC, Bipath P, Hlophe YN. Chemokines as possible therapeutic targets in metastatic melanoma. Cancer Medicine. 2023; 12: 14387–14402. https://doi.org/10.1002/cam4.6055

[37] Vergani E, Di Guardo L, Dugo M, Rigoletto S, Tragni G, Ruggeri R, et al. Overcoming melanoma resistance to vemurafenib by targeting CCL2-induced miR-34a, miR-100 and miR-125b. Oncotarget. 2016; 7: 4428–4441. https://doi.org/10.18632/oncotarget.6599

[38] Wang CH, Wang LK, Tsai FM. A Novel Role for Tazarotene-induced Gene 1 in Suppressing Melanoma Growth - Schlafen 11. Frontiers in Bioscience (Landmark Edition). 2025; 30: 37895. https://doi.org/10.31083/FBL37895

[39] Chen X, Cubillos-Ruiz JR. Endoplasmic reticulum stress signals in the tumour and its microenvironment. Nature Reviews. Cancer. 2021; 21: 71–88. https://doi.org/10.1038/s41568-020-00312-2

[40] Xu F, Wang L. Deciphering ER stress-unfolded protein response relationship by visualizing unfolded proteins in the ER. Cell Reports. 2024; 43: 114358. https://doi.org/10.1016/j.celrep.2024.114358
[41] Yu X, Li W, Sun S, Li J. Endoplasmic Reticulum Stress in Cancer Progression: A Comprehensive Review of Its Role and Mechanisms. International Journal of Medical Sciences. 2025; 22: 4561–4585. https://doi.org/10.7150/ijms.120874
[42] Zhang W, Shi Y, Oyang L, Cui S, Li S, Li J, et al. Endoplasmic reticulum stress-a key guardian in cancer. Cell Death Discovery. 2024; 10: 343. https://doi.org/10.1038/s41420-024-02110-3
[43] Ong G, Ragetli R, Mnich K, Doble BW, Kammouni W, Logue SE. IRE1 signaling increases PERK expression during chronic ER stress. Cell Death & Disease. 2024; 15: 276. https://doi.org/10.1038/s41419-024-06663-0
[44] Liu L, Yao D, Chen Z, Duan S. A comprehensive signature based on endoplasmic reticulum stress-related genes in predicting prognosis and immunotherapy response in melanoma. Scientific Reports. 2023; 13: 8232. https://doi.org/10.1038/s41598-023-35031-9
[45] Hersey P, Zhang XD. Adaptation to ER stress as a driver of malignancy and resistance to therapy in human melanoma. Pigment Cell & Melanoma Research. 2008; 21: 358–367. https://doi.org/10.1111/j.1755-148X.2008.00467.x
[46] Kong Y, Jiang J, Huang Y, Li L, Liu X, Jin Z, et al. Endoplasmic reticulum stress in melanoma pathogenesis and resistance. Biomedicine & Pharmacotherapy = Biomedecine & Pharmacotherapie. 2022; 155: 113741. https://doi.org/10.1016/j.biopha.2022.113741
[47] Cerezo M, Lehraiki A, Millet A, Rouaud F, Plaisant M, Jaune E, et al. Compounds Triggering ER Stress Exert Anti-Melanoma Effects and Overcome BRAF Inhibitor Resistance. Cancer Cell. 2016; 29: 805–819. https://doi.org/10.1016/j.ccell.2016.04.013
[48] Ho DV, Chan JY. Induction of Herpud1 expression by ER stress is regulated by Nrf1. FEBS Letters. 2015; 589: 615–620. https://doi.org/10.1016/j.febslet.2015.01.026
[49] Zinszner H, Kuroda M, Wang X, Batchvarova N, Lightfoot RT, Remotti H, et al. CHOP is implicated in programmed cell death in response to impaired function of the endoplasmic reticulum. Genes & Development. 1998; 12: 982–995. https://doi.org/10.1101/gad.12.7.982
[50] Oyadomari S, Mori M. Roles of CHOP/GADD153 in endoplasmic reticulum stress. Cell Death and Differentiation. 2004; 11: 381–389. https://doi.org/10.1038/sj.cdd.4401373
[51] Hosomi S, Grootjans J, Huang YH, Kaser A, Blumberg RS. New Insights Into the Regulation of Natural-Killer Group 2 Member D (NKG2D) and NKG2D-Ligands: Endoplasmic Reticulum Stress and CEA-Related Cell Adhesion Molecule 1. Frontiers in Immunology. 2018; 9: 1324. https://doi.org/10.3389/fimmu.2018.01324
[52] Raulet DH, Marcus A, Coscoy L. Dysregulated cellular functions and cell stress pathways provide critical cues for activating and targeting natural killer cells to transformed and infected cells. Immunological Reviews. 2017; 280: 93–101. https://doi.org/10.1111/imr.12600
[53] Chan CJ, Smyth MJ, Martinet L. Molecular mechanisms of natural killer cell activation in response to cellular stress. Cell Death and Differentiation. 2014; 21: 5–14. https://doi.org/10.1038/cdd.2013.26
[54] Cubillos-Ruiz JR, Silberman PC, Rutkowski MR, Chopra S, Perales-Puchalt A, Song M, et al. ER Stress Sensor XBP1 Controls Anti-tumor Immunity by Disrupting Dendritic Cell Homeostasis. Cell. 2015; 161: 1527–1538. https://doi.org/10.1016/j.cell.2015.05.025
[55] Mahadevan NR, Rodvold J, Sepulveda H, Rossi S, Drew AF, Zanetti M. Transmission of endoplasmic reticulum stress and pro-inflammation from tumor cells to myeloid cells. Proceedings of the National Academy of Sciences of the United States of America. 2011; 108: 6561–6566. https://doi.org/10.1073/pnas.1008942108